

**A dynamic plant chamber system with downstream reaction chamber**

J. Timkovsky et al.

**A dynamic plant chamber system with downstream reaction chamber to study the effects of pollution on biogenic emissions**

**J. Timkovsky<sup>1</sup>, P. Gankema<sup>2</sup>, R. Pierik<sup>2</sup>, and R. Holzinger<sup>1</sup>**

<sup>1</sup>Institute for Marine and Atmospheric Research Utrecht, Utrecht University, Utrecht, the Netherlands

<sup>2</sup>Plant Ecophysiology, Institute of Environmental Biology, Utrecht University, the Netherlands

Received: 30 September 2013 – Accepted: 12 October 2013 – Published: 22 October 2013

Correspondence to: J. Timkovsky (j.timkovsky@uu.nl)

Published by Copernicus Publications on behalf of the European Geosciences Union.

Title Page

Abstract

Introduction

Conclusions

References

Tables

Figures

⏪

⏩

◀

▶

Back

Close

Full Screen / Esc

Printer-friendly Version

Interactive Discussion

## Abstract

A system of two dynamic plant chambers and a downstream reaction chamber has been set up to investigate the emission of biogenic volatile organic compounds (BVOC) and possible effects from pollutants such as ozone. The system can be used to compare BVOC emissions from two sets of differently treated plants, or to study the photochemistry of real plant emissions under polluted conditions without exposing the plants to pollutants. The main analytical tool is a proton-transfer-reaction time-of-flight mass spectrometer (PTR-TOF-MS) which allows online monitoring of biogenic emissions and chemical degradation products. The identification of BVOCs and their oxidation products is aided by cryogenic trapping and subsequent in situ gas chromatographic analysis. The data presented in the paper demonstrates the good performance of the setup.

## 1 Introduction

Volatile organic compounds (VOC) are reactive substances in the atmosphere which have a strong impact on atmospheric chemistry (Fehsenfeld et al., 1992; Riipinen et al., 2011; Sahu, 2012). Biogenic volatile organic compound (BVOC) emissions constitute approximately 90 % of global VOC emissions which are estimated to be  $1150 \text{ TgCyr}^{-1}$  (Guenther et al., 2006). Oxidation of BVOCs in the atmosphere in the presence of  $\text{NO}_x$  leads to the formation of ozone. Tropospheric ozone is a greenhouse gas and a strong oxidant which makes it harmful for living organisms (Summerfelt and Hochheimer, 1997; Denman et al., 2007). Moreover, oxidation products of BVOCs contribute to secondary organic aerosol (SOA) formation through condensation on existing particles or the formation of new particles (Kulmala, 2003; Goldstein and Galbally, 2007). Aerosols and ozone can penetrate into the lungs of humans thus causing long- and short-term health effects (Harrison and Yin, 2000). Furthermore, aerosols and ozone have an impact on Earth's climate: ozone is a strong greenhouse gas and aerosols

## A dynamic plant chamber system with downstream reaction chamber

J. Timkovsky et al.

Title Page

Abstract

Introduction

Conclusions

References

Tables

Figures

⏪

⏩

◀

▶

Back

Close

Full Screen / Esc

Printer-friendly Version

Interactive Discussion



scatter and/or absorb solar radiation. Aerosols also influence the climate indirectly by serving as cloud-condensation nuclei (Andreae and Crutzen, 1997).

While BVOCs are known to affect the atmosphere and human health, much remains unknown about how atmospheric pollutants affect plant VOC emissions. Increased ozone levels may increase or decrease BVOC emissions, depending on plant species and environmental conditions. For example, Beauchamp et al. (2005) showed that C6-volatile emissions increased after ozone exposure in tobacco plants, while Hartikainen et al. (2012) showed decreased VOC emissions upon elevated ozone levels in birch trees. In addition, Karl et al. (2010) showed that pollutants like oxygenated VOCs can be removed by plants through dry deposition. At the same time it is not understood how such deposition influences the ability of plants to emit BVOCs (Karl et al., 2010). Plant VOC emissions are affected by many environmental factors, including abiotic factors like temperature and light as well as biotic factors like herbivores, pathogens and neighboring plants (Niinements, 2010; Guenther et al., 2000; Sharkey and Loreto, 1993; Kegge and Pierik, 2010).

Here we present a setup of dynamic plant chambers and a reaction chamber, which can be used to study interactions between BVOC emissions and pollution. The main features include automated operation to study real plant emissions under different environmental conditions. BVOC analysis is based on proton-transfer-reaction time-of-flight mass spectrometry (PTR-TOF-MS) which allows precise online measurements of different VOCs in the air with high mass resolution (Jordan et al., 2009; Graus et al., 2010). In addition, the PTR-TOF-MS is coupled to a gas chromatograph (GC) system in order to improve the identification of isomers (e.g. different monoterpenes). Results from an ozonolysis experiment with  $\beta$ -pinene and three experiments with birch (*Betula pendula*) seedlings (referred to as experiment A, B, and C) are shown here to demonstrate the performance of the system.

## A dynamic plant chamber system with downstream reaction chamber

J. Timkovsky et al.

Title Page

Abstract

Introduction

Conclusions

References

Tables

Figures

⏪

⏩

◀

▶

Back

Close

Full Screen / Esc

Printer-friendly Version

Interactive Discussion



## 2 Description of the setup

The schematic setup of the system is shown in Fig. 1. Two optional chamber setups are shown in charts A and B. Chart C shows how the PTR-TOF-MS is connected to the different sampling ports of the chamber system, and chart D shows the functioning of the GC system.

### 2.1 The plant and reaction chambers system

As plant chambers we use two desiccators with a volume of 25 L each. The desiccators are identical and consist of three parts: the cap, the desiccator body and the hose, which is located in the cap. The hose has a long outlet ( $l = 25$  cm, ID = 9 mm), which is directed towards the bottom of the desiccator and allows sampling from the center of the plant chamber. The gas inlet to the chamber is located at the top of the hose.

The custom-made reaction chamber is made from perfluoroalkoxy film (PFA, thickness 0.05 mm, HP Products, the Netherlands) and has a cylindrical shape. The walls were sealed by welding the PFA film with a heat gun (Steinel, Germany). The physical characteristics of the reaction chamber are the following: diameter = 45 cm, height = 50 cm, volume = 80 L. The bottom of the chamber is fixed to a ground plate covered with a PFA film. The axle of a polytetrafluoroethylene ventilator (PTFE, OD = 10 mm, Bola, Germany) is lead through the center of the ground plate, the ventilator is positioned in the center of the chamber. Operating the ventilator at 2 Hz keeps the chamber well mixed during the experiments. All mounting parts in contact with the air inside the reaction chamber were made from Teflon (PTFE). The tightness of the reaction chamber was tested by filling the chamber with acetone at levels of several hundred  $\text{nmol mol}^{-1}$  and monitoring the mixing ratio without gas flow through the chamber. No significant leaks were detected.

The flow through the plant chambers can be controlled by thermal mass-flow controllers (MKS Instruments, Germany) in the range 0–20 and 0–5 standard  $\text{L min}^{-1}$  (standard is referring to standard conditions: 1013.25 hPa, 273.15 K) for chamber 1

## A dynamic plant chamber system with downstream reaction chamber

J. Timkovsky et al.

Title Page

Abstract

Introduction

Conclusions

References

Tables

Figures

⏪

⏩

◀

▶

Back

Close

Full Screen / Esc

Printer-friendly Version

Interactive Discussion



and 2, respectively. During all experiments the flow through both plant chambers was  $2.5 \text{ L min}^{-1}$ . We used pressurized (5 bars) ambient air which was purified through a custom made charcoal filter. The charcoal was cleaned once a week by removing the charcoal from the tube and placing it overnight in an oven at  $160^\circ\text{C}$ .

In the “dual plant chamber” setup (Fig. 1a) the sampling ports are located directly at the outlets of the plant chambers and a third sampling port is located after the charcoal filter to monitor the incoming air. In the “reaction chamber” setup (Fig. 1b) the sampling ports are located directly after the reaction chamber, after the plant chambers, and after the charcoal filter. Relative humidity and temperature sensors (HMP 60, Vaisala, Finland) are located at the outlets to monitor humidity and temperature in all chambers.

We used Teflon (PFA) tubing to connect the plant chambers, the reaction chamber, and instruments (length between plant and reaction chamber = 145 cm, ID = 9 mm). Defined amounts of ozone can be added before plant chamber 1 (Fig. 1a) or the reaction chamber (Fig. 1b) with an ozone generator (Model 49i-PS, Thermo Scientific, US). This is done by turning on the generator (set to  $1500 \text{ nmol mol}^{-1}$ ) and switching valve 3. The ozone addition to the plant chamber 1 and the reaction chamber is controlled with a thermal mass-flow controller (MKS, Germany) in the range  $0\text{--}2 \text{ L min}^{-1}$ . Ozone is monitored ( $\text{O}_3$  analyzer model 49 W003 Thermo Environmental Instruments Inc., USA) at the outlet of either plant chamber 1 or the reaction chamber.

An array of nine 36W/840 TL-D lamps (Philips, the Netherlands) above the plant chambers is used to produce light levels of  $130\text{--}150 \mu\text{mol m}^{-2} \text{ s}^{-1}$  photosynthetically active radiation (PAR:  $\lambda = 400\text{--}700 \text{ nm}$ ) at the center of the plant chambers when the lid was closed.

## 2.2 Analytical tools

### 2.2.1 PTR-TOF-MS

Figure 1c shows how the PTR-TOF-MS is switched between the three sampling ports of the chamber system, the effluent of the GC column (the PTR-TOF-MS is also used

## A dynamic plant chamber system with downstream reaction chamber

J. Timkovsky et al.

Title Page

Abstract

Introduction

Conclusions

References

Tables

Figures

⏪

⏩

◀

▶

Back

Close

Full Screen / Esc

Printer-friendly Version

Interactive Discussion



as detector for the GC system), and laboratory air, which can be routinely monitored as well. This valve system is implemented with 1/8" PFA tubing, four 2-way and two 3-way Teflon (PFA) solenoid valves (TEQCOM, port size 1/8", orifice 0.125).

We use a standard PTR-TOF-MS (Ionicon Inc., Austria), which has been described by Jordan et al. (2009), with the following parameters: temperature of the drift tube, 60 °C; temperature of the inlet tube, 60 °C; drift tube pressure, 2.15 hPa; ion source voltages,  $U_s = 140$  V,  $U_{so} = 92$  V; E/N, 134 Td; extraction voltage at the end of the drift tube,  $U_{dx} = 35$  V. The ion source current is kept between 5 and 7 mA and we provide a water flow of 4 standard mL min<sup>-1</sup> to the ion source. At the normal operational conditions the intensity of the primary signal (detected at  $m/z$  21.023) is around 500–2000 cps. However, during the experiments B and C the primary signal was low (~ 100–200 cps), whereas during experiment A the primary signal was at its normal level (~ 500 cps). During the ozonolysis of  $\beta$ -pinene experiment the primary signal was ~ 200 cps.

The settings of the TOF are such that every 60 microseconds a pulse of ions is injected into the mass spectrometer, which corresponds to a mass range of 0–1165 Th. 16 667 of these initial mass spectra are averaged and saved to one mass scan which corresponds to a time resolution of one second. The mass resolution ( $m/\Delta m$ , where  $\Delta m$  is the full width at half maximum) is typically in the range of 3500–5000. Data processing is done with Interactive Data Language (IDL, version 7.0.0, ITT Visual Information Solutions), using custom made routines described by Holzinger et al. (2010a).

Mixing ratios of most compounds were calculated according to the method described in Holzinger et al. (2010b), which involves the use of default reaction rate constants ( $3 \times 10^{-9}$  cm<sup>3</sup> s<sup>-1</sup> molecule<sup>-1</sup>), default transmission efficiencies, and calculated reaction times. The accuracy of the calculated mixing ratios should be better than 50 % for most compounds (Holzinger et al., 2010b). In addition, gas standards were used to calibrate the mixing ratios of monoterpenes, acetaldehyde and acetone with an accuracy of 17 %, calculated as the sum of the precision of PTR-TOF-MS and the accuracy of the gravimetrically mixed calibration standard.

## A dynamic plant chamber system with downstream reaction chamber

J. Timkovsky et al.

Title Page

Abstract

Introduction

Conclusions

References

Tables

Figures

⏪

⏩

◀

▶

Back

Close

Full Screen / Esc

Printer-friendly Version

Interactive Discussion







## 2.4 Operation of the system

To demonstrate the operation of the system, Fig. 2 shows the course of the mixing ratios detected at  $m/z$  81.069 ( $C_6H_9^+$  fragment) for one cycle of experiment A. The PTR-TOF-MS was switched between the different ports to measure as follows (see Fig. 2): for 10 min reaction chamber air, for 5 min purified air, for 10 min plant chambers air, for 25.5 min GC effluent, for 10 min plant chambers air, for 36 min reaction chamber air (ozone addition to the reaction chamber happens during this period), for 25.5 min GC effluent, for 5 min lab air. Thereafter, new two-hour cycles were started automatically.

The periods of GC sampling (7 min each) are also indicated in Fig. 2. Ozone addition lasted for 17 min (see blue bracket in Fig. 2) and GC sampling was performed during the last 7 min of the ozone treatment.

The following periods (indicated in Fig. 2 by the respective lines below the  $x$  axis) were used for averaging/integration: last 7 min of non-ozonated reaction chamber air measurements, last 4 min of purified air measurements, last 9 min of first plant chamber air measurements, first 15 min of first GC chromatogram, last 4 min of second plant chamber air measurements, last 7 min of ozonated reaction chamber air measurements, first 15 min of second GC chromatogram.

## 2.5 Experiments performed

### 2.5.1 Ozonolysis of $\beta$ -pinene

During this experiment flow through the reaction chamber was maintained at  $7 \text{ L min}^{-1}$  by two flow controllers which were set to 5 and  $2 \text{ L min}^{-1}$ , respectively. This resulted in an air residence time of 11.5 min in the reaction chamber. The larger flow contained  $\sim 350 \text{ nmol mol}^{-1}$  of  $\beta$ -pinene, which was produced by diluting a small flow ( $20 \text{ mL min}^{-1}$ ) of headspace air from a flask with liquid  $\beta$ -pinene (Sigma Aldrich, 99%) into the larger

## A dynamic plant chamber system with downstream reaction chamber

J. Timkovsky et al.

Title Page

Abstract

Introduction

Conclusions

References

Tables

Figures

◀

▶

◀

▶

Back

Close

Full Screen / Esc

Printer-friendly Version

Interactive Discussion

flow of purified air. Ozone levels of  $\sim 1.3 \mu\text{mol mol}^{-1}$  were produced in the 2 L flow by the ozone generator.

## 2.5.2 Birch seedling experiments

Experiment A was performed on 4–5 August 2012, experiment B – on 22–23 August 2012 and experiment C – on 24–25 August 2012. Birch (*Betula pendula*) seedlings were collected with their surrounding sandy soil from a forest close to the Utrecht University campus 1–2 days before the experiments, and placed in 250 mL pots. The seedlings were 1–2 yr old. Due to weather conditions, the soil of seedlings used in experiment C was very dry. After transfer to the lab, the seedlings were placed next to the plant chambers, where the TL-D lamps produced light levels of  $130\text{--}150 \mu\text{mol m}^{-2} \text{s}^{-1}$  PAR with a light period from 07:00 till 23:00 LT (16 h light, 8 h dark). Day and night temperatures were  $21.5 \pm 0.2$  and  $20.2 \pm 0.2$  °C, respectively. Relative humidity was 40–60 %. Three plants were put into each plant chamber. After the lids were closed the air flow of  $2.5 \text{ L min}^{-1}$  was maintained for 30 min before the start of the experiment to allow plant emissions to stabilize.

After the experiment, leaves were harvested, fresh weight was measured and leaf area was determined with a Li-3100 Area Meter (Lincoln, Nebraska, USA). Dry weight was measured after placing the leaves in an oven at 70 °C for at least 48 h.

Before experiments B and C, the reaction chamber was pre-cleaned overnight by being flushed with purified air containing ozone mixing ratios of  $\sim 430 \text{ nmol mol}^{-1}$ . To check if chambers were clean, background measurements (with purified air) of empty plant and reaction chambers were made. The experiments were performed according to the measurement cycle described in Sect. 2.4.

Emission rates (ER) of the birch seedlings were calculated according to Eq. (1):

$$\text{ER} = \frac{[\text{VOC}] \cdot M_{\text{VOC}} \cdot F_{\text{cham}}}{\text{DW}} \quad (1)$$

## A dynamic plant chamber system with downstream reaction chamber

J. Timkovsky et al.

Title Page

Abstract

Introduction

Conclusions

References

Tables

Figures

⏪

⏩

◀

▶

Back

Close

Full Screen / Esc

Printer-friendly Version

Interactive Discussion











$\beta$ -pinene and ozone mixing ratios, and/or (iii) the absence of an OH scavenger which would lead to a longer time for the system to reach equilibrium.

In addition to known compounds, several other compounds were observed, which had not been described previously. For the single experiment reported here we cannot exclude the possibility that these products were artifacts from wall contamination. Nevertheless, these newly observed compounds show the potential of the setup to identify more products of the oxidation of  $\beta$ -pinene, when improved cleaning protocols are followed and background measurements are performed. Finally, we observed that mixing ratios of sticky compounds like formic acid ( $m/z$  47.013) increased slower in the reaction chamber than other compounds (Fig. 5), indicating that a fraction of these products are lost to the walls of the reaction chamber. However, the loss is limited and towards the end of the experiment ( $\sim 300$  min, Fig. 5) the gas phase levels of  $m/z$  47.013 were in equilibrium.

### 3.2 Emission rates of birch seedlings

In each experiment, the plants in the plant chambers had a total dry weight of 4.1–5.3 g, and a total leaf area of 1296–1413 cm<sup>2</sup>. All reported compounds were emitted during the day and many of them during the night, with daytime emissions being 1.8–3.2 times higher than nighttime emissions (Table 3). Increased emissions of BVOCs during the day and upon exposure to increased light intensity were reported before in several plant species including lima bean, cotton and poplar (Loughrin et al., 1994; Loivamäki et al., 2007; Arimura et al., 2008). A broad spectrum of the emitted compounds was observed indicating the good sensitivity of the system even towards the compounds emitted in low quantities during the day as well as during the night. For several compounds emitted during the day no emissions at night were observed.

## A dynamic plant chamber system with downstream reaction chamber

J. Timkovsky et al.

Title Page

Abstract

Introduction

Conclusions

References

Tables

Figures

⏪

⏩

◀

▶

Back

Close

Full Screen / Esc

Printer-friendly Version

Interactive Discussion

### 3.3 Ozonolysis of birch emissions

Figure 6 shows the course of the measured ozone and monoterpene mixing ratios. Minimum monoterpene mixing ratios and maximum ozone mixing ratios were observed at the same time in the reaction chamber demonstrating that chemical reactions with ozone were the cause of monoterpenes depletion (Atkinson and Arey, 2003). We modeled the monoterpene mixing ratios in the reaction chamber during the period shown in Fig. 6 in order to check if the degradation rate of monoterpenes was in agreement with the measured ozonolysis rate constants of the observed monoterpenes emitted from the birch seedlings. The initial monoterpenes mixing ratio, the mixing ratio of ozone, and first order kinetics were used. The initial monoterpenes mixing ratio was attributed to individual monoterpenes by using the information from the chromatogram shown in Fig. 4d. The relative fractions were 0.28, 0.47, and 0.25 for  $\alpha$ -pinene, d-limonene, and  $\beta$ -phellandrene, respectively. The reaction rates for these compounds with ozone have been measured to be  $8.7 \times 10^{-17}$ ,  $2.0 \times 10^{-16}$  and  $4.8 \times 10^{-17} \text{ cm}^3 \text{ molec}^{-1} \text{ s}^{-1}$ , respectively (Atkinson, 1997; Shorees et al., 1991). Using this information the degradation of the monoterpenes was calculated separately and the total monoterpene mixing ratio at every time step was calculated as the sum of the individual contributions. The measured and modeled monoterpene mixing ratios (see Fig. 6) agree reasonably well, showing that the general description of the observed chemistry in the reaction chamber is adequate. Somewhat lower measured monoterpene mixing ratios in comparison to the calculated values were associated with the absence of an OH scavenger in the system which could lead to a faster monoterpene degradation due to reactions with the OH radical.

Figure 7 shows averaged monoterpene mixing ratios measured online in the reaction chamber before and after ozone addition in experiment B. The decrease of monoterpene signal during/after ozonolysis as shown in Fig. 6 and described above was well reproducible. Due to the low primary signal the sensitivity of the instrument during experiment B was rather low which caused the detection of only few ions produced during

## A dynamic plant chamber system with downstream reaction chamber

J. Timkovsky et al.

Title Page

Abstract

Introduction

Conclusions

References

Tables

Figures

⏪

⏩

◀

▶

Back

Close

Full Screen / Esc

Printer-friendly Version

Interactive Discussion

## A dynamic plant chamber system with downstream reaction chamber

J. Timkovsky et al.

Title Page

Abstract

Introduction

Conclusions

References

Tables

Figures

⏪

⏩

◀

▶

Back

Close

Full Screen / Esc

Printer-friendly Version

Interactive Discussion

the ozonolysis. Despite the reasonable understanding of the chemistry happening in the reaction chamber it was difficult to identify ozonolysis products from experiments A–C. The reaction chamber was not well cleaned before the start of experiment A and ozonolysis products were also from contamination, i.e. reactive organic species sticking to the walls of the reaction chamber system. For example, during experiment A the production of  $m/z$  61.029 (calculated as a difference in mixing ratios for an ion in the reaction chamber with and without ozone added) during the night was higher than during the following day, despite much lower monoterpene levels during the night. This indicated a significant contribution from contamination to the signal of the ion, and in experiment A a similar behavior was observed for many other ions. In the experiments B and C the proper cleaning procedure was applied, therefore the abovementioned problems were not encountered. The change in monoterpenes mixing ratio upon the ozone addition was below the detection limit of PTR-TOF-MS due to very low plant emissions in experiment C. Therefore, it was not possible to calculate the yields for experiment C and apply the filter (a) described in Sect. 2.7.

In order to overcome these issues the filters mentioned in Sect. 2.7 were developed. Initially we detected 193 ions during experiments A, B and C. Of these, 43 and 60 ions passed the Student's  $t$  test in experiment A and B, respectively. None of the 43 ions from experiment A and only 2 ions from the 60 ions from experiment B passed the additional filters (a) and (b):  $m/z$  47.048 (corresponding to the molecular formula  $C_2H_7O^+$ ) with a molar yield  $25.9 \pm 9.8\%$  and  $m/z$  73.029 (corresponding to the molecular formula  $C_3H_5O_2^+$ ) with a molar yield  $29.5 \pm 8.2\%$ .

Despite the low number of detected ozonolysis products, the above mentioned experiments demonstrated the capability of the system to detect ozonolysis products even at low mixing ratios of the parent compounds which can be improved by better reaction chamber pre-cleaning protocols and better (standard) PTR-TOF-MS performance, in which case the number of ions removed by filters (a) and (b) would be much reduced.

## 4 Conclusions

The setup to measure impact of pollution on plant emissions was tested and first results are reported here. In the  $\beta$ -pinene ozonolysis experiment the expected products were observed, although with somewhat lower yields than described in the literature. In the experiments with real plant emissions, mixing ratios in the plant chambers and the reaction chamber are shown to coincide, showing good quantitative transfer of the VOCs between these components of the setup. This shows a good performance of the plant chamber and the reaction chamber setup, including ozone addition and online VOC measurements.

The sampling efficiency of the GC system has been tested. The recovery factors were within the range of 0.71–1.38, indicating that cryogenic sampling and the transfer through the GC system is adequate. The added value of the GC part of the system was clear from the analysis of birch seedling emissions, where it allowed us to distinguish three specific monoterpenes within the birch monoterpene emissions.

We performed experiments with birch seedlings and found emission of 14 species. As expected, birch emission rates were higher during the day than during the night (1.8–3.2 fold higher), and for several of these species no nighttime emissions could be detected.

Addition of ozone to the birch seedling emissions resulted in decreased monoterpene mixing ratios. The modeled monoterpene mixing ratios in the reaction chamber agreed reasonably well with the measured levels. Our results show that our setup is capable of detecting ozonolysis products at low levels ( $< 1 \text{ nmol mol}^{-1}$ ) of biogenic emissions, although relatively few ozonolysis products were observed. Comparison of experiment A with B and C shows that proper cleaning protocols are essential.

The flexibility of the setup provides the possibility to perform a broad spectrum of experiments. The full automatization of the system allows easy-to-perform long- and short-term measurements. Therefore, the presented setup is a valuable tool to study the effects of pollution on plant emissions.

## A dynamic plant chamber system with downstream reaction chamber

J. Timkovsky et al.

Title Page

Abstract

Introduction

Conclusions

References

Tables

Figures



Back

Close

Full Screen / Esc

Printer-friendly Version

Interactive Discussion

*Acknowledgements.* The TD-PTR-MS has been funded by the Netherlands Organization for Scientific Research (NWO) under the ALW-Middelgroot program (Grant 834.08.002). This project is funded by a strategic funding scheme (Focus and Mass) of Utrecht University. We would like to thank Carina van der Veen, Henk Snellen, Michel Bolder and Marcel Portanger of Utrecht University, the Netherlands for the excellent technical support and Rens Voeselek and Thomas Röckmann for scientific discussion.

## References

- Andreae, M. O. and Crutzen, P. J.: Atmospheric aerosols: biogeochemical sources and role in atmospheric chemistry, *Science*, 276, 1052–1058, 1997.
- Arey, J., Atkinson, R., and Aschmann, S. M.: Product study of the gas-phase reactions of monoterpenes with the OH radical in the presence of NO<sub>x</sub>, *J. Geophys. Res.*, 95, 18539–18546, 1990.
- Arimura, G., Köpke, S., Kunert, M., Volpe, V., David, A., Brand, P., Dabrowska, P., Maffei, M. E., and Boland, W.: Effects of feeding *Spodoptera littoralis* on lima bean leaves: IV. Diurnal and nocturnal damage differentially initiate plant volatile emission, *Plant Physiol.*, 146, 965–973, 2008.
- Atkinson, R.: Gas-phase tropospheric chemistry of volatile organic compounds: 1. Alkanes and alkenes, *J. Phys. Chem. Ref. Data*, 26, 215–290, 1997.
- Atkinson, R. and Arey, J.: Gas-phase tropospheric chemistry of biogenic volatile organic compounds: a review, *Atmos. Environ.*, 37, 197–219, doi:10.1016/S1352-2310(03)00391-1, 2003.
- Beauchamp, J., Wisthaler, A., Hansel, A., Kleist, E., and Miebach, M.: Ozone induced emissions of biogenic VOC from tobacco: relationships between ozone uptake and emission of LOX products Volatile organic compound (VOC) emissions from tobacco, *Plant Cell Environ.*, 28, 1334–1343, 2005.
- Denman, K. L., Brasseur, G., Chidthaisong, A., Ciais, P., Cox, P. M., Dickinson, R. E., Hauglustaine, D., Heinze, C., Holland, E., Jacob, D., Lohmann, U., Ramachandran, S., da Silva Dias, P. L., Wofsy, S. C., and Zhang, X.: Climate Change 2007: The Physical Science Basis, Contribution of Working Group I to the Fourth Assessment Report of the Intergovernmental Panel on Climate Change; New York: Cambridge University Press, 2007.

## A dynamic plant chamber system with downstream reaction chamber

J. Timkovsky et al.

Title Page

Abstract

Introduction

Conclusions

References

Tables

Figures



Back

Close

Full Screen / Esc

Printer-friendly Version

Interactive Discussion





**A dynamic plant chamber system with downstream reaction chamber**

J. Timkovsky et al.

Title Page

Abstract

Introduction

Conclusions

References

Tables

Figures

◀

▶

◀

▶

Back

Close

Full Screen / Esc

Printer-friendly Version

Interactive Discussion

novel high mass resolution thermal-desorption proton-transfer-reaction mass-spectrometer (hr-TD-PTR-MS), *Atmos. Chem. Phys.*, 10, 10111–10128, doi:10.5194/acp-10-10111-2010, 2010a.

Holzinger, R., Williams, J., Herrmann, F., Lelieveld, J., Donahue, N. M., and Röckmann, T.: Aerosol analysis using a Thermal-Desorption Proton-Transfer-Reaction Mass Spectrometer (TD-PTR-MS): a new approach to study processing of organic aerosols, *Atmos. Chem. Phys.*, 10, 2257–2267, doi:10.5194/acp-10-2257-2010, 2010b.

Jaoui, M. and Kamens. R. M.: Mass balance of gaseous and particulate products from beta-pinene/O<sub>3</sub>/air in the absence of light and beta-pinene/NO<sub>x</sub>/air in the presence of natural sunlight, *J. Atmos. Chem.*, 45, 101–141, 2003.

Jordan, A., Haidacher, S., Hanel, G., Hartungen, E., Märk, L., Seehauser, H., Schottkowsky, R., Sulzer, P., and Mark, T. D.: A high resolution and high sensitivity proton-transfer-reaction time-of-flight mass spectrometer (PTR-TOF-MS), *Int. J. Mass Spectrom.*, 286, 122–128, doi:10.1016/j.ijms.2009.07.005, 2009.

Karl, T., Harley, P., Emmons, L., Thornton, B., Guenther, A., Basu, C., Turnipseed, A., and Jardine, K.: Efficient atmospheric cleansing of oxidized organic trace gases by vegetation, *Science*, 330, 816–819, doi:10.1126/science.1192534, 2010.

Kegge, W. and Pierik, R.: Biogenic volatile organic compounds and plant competition, *Trends Plant Sci.*, 15, 126–132, doi:10.1016/j.tplants.2009.11.007, 2009.

König, G., Brunda, M., Puxbaum, H., Hewitt, C. N., Duckham, S. C., and Rudolph, J.: Relative contribution of oxygenated hydrocarbons to the total biogenic VOC emissions of selected mid-European agricultural and natural plant species, *Atmos. Environ.*, 29, 861–874, 1995.

Kulmala, M.: How particles nucleate and grow, *Science*, 302, 1000–1001, doi:10.1126/science.1090848, 2003.

Larsen, B. R., Di Bella, D., Glasius, M., Winterhalter, R., Jensen, N. R., and Hjorth, J.: Gas-phase OH oxidation of monoterpenes: gaseous and particulate products, *J. Atmos. Chem.*, 38, 231–276, 2001.

Leblanc, D. C.: *Statistics – Concepts and Applications for Science*, 189, Jones and Bartlett, Sudbury, MA, 2004.

Lee, A., Goldstein, A. H., Kroll, J. H., Ng, N. L., Varutbangkul, V., Flagan, R. C., and Seinfeld, J. H.: Gas-phase products and secondary aerosol yields from the photooxidation of 16 different terpenes, *J. Geophys. Res.*, 111, D17305, doi:10.1029/2006JD007050, 2006.



## A dynamic plant chamber system with downstream reaction chamber

J. Timkovsky et al.

**Table 1.** Recovery factors (RF) for several compounds, calculated from experiment A, B and C using Eq. (3). All chromatograms that sampled from the ozone free reaction chamber have been included into this analysis ( $n = 40$ ). Numbers shown are averages  $\pm$  SD.

Compound or $m/z$	Formula $H^+$	RF $\pm$ SD
33.033	$CH_4OH^+$	$0.75 \pm 0.10$
43.018	$C_2H_3O^+$	$0.82 \pm 0.07$
59.049	$C_3H_7O^+$	$0.71 \pm 0.08$
61.029	$C_2H_5O_2^+$	$1.38 \pm 0.26$
69.07	$C_5H_9^+$	$1.09 \pm 0.28$
87.045	$C_4H_7O_2^+$	$1.10 \pm 0.16$
87.081	$C_5H_{11}O^+$	$1.20 \pm 0.25$
monoterpenes	$C_{10}H_{17}^+$	$1.23 \pm 0.31$

Title Page

Abstract

Introduction

Conclusions

References

Tables

Figures

⏪

⏩

◀

▶

Back

Close

Full Screen / Esc

Printer-friendly Version

Interactive Discussion

## A dynamic plant chamber system with downstream reaction chamber

J. Timkovsky et al.

Title Page

Abstract

Introduction

Conclusions

References

Tables

Figures

◀

▶

◀

▶

Back

Close

Full Screen / Esc

Printer-friendly Version

Interactive Discussion

**Table 2.** Molar yields of ozonolysis products of  $\beta$ -pinene obtained in this study and in the literature (Lee et al., 2006<sup>a</sup>; Arey et al., 1990<sup>b</sup>; Hatakeyama et al., 1991<sup>c</sup>; Jaoui and Kamens, 2003<sup>d</sup>; Larsen et al., 2001<sup>e</sup>; Orlando et al., 2000<sup>f</sup>; Wisthaler et al., 2001<sup>g</sup>).

Product	<i>m/z</i>	Formula H <sup>+</sup>	Yield, % [literature]	Yield, % [this work]
formaldehyde	31.018	CH <sub>3</sub> O <sup>+</sup>	23 <sup>e</sup> –54 <sup>c</sup>	5.9
	33.033	CH <sub>4</sub> OH <sup>+</sup>		0.35
	41.038	C <sub>3</sub> H <sub>5</sub> <sup>+</sup>		0.53
	43.018	C <sub>2</sub> H <sub>3</sub> O <sup>+</sup>		4.17
acetaldehyde	45.033	C <sub>2</sub> H <sub>4</sub> O	0.6 <sup>a</sup>	1.07
formic acid	47.013	HCOOH <sub>2</sub> <sup>+</sup>	2.0 <sup>f</sup> –38.0 <sup>e</sup>	1.76
	47.022	no match		0.42
acetone	59.049	C <sub>3</sub> H <sub>7</sub> O <sup>+</sup>	2.0 <sup>f</sup> –16.0 <sup>g</sup>	16.90
acetic acid	61.029	C <sub>2</sub> H <sub>5</sub> O <sub>2</sub> <sup>+</sup>	1.4 <sup>a</sup>	0.98
	73.029	C <sub>3</sub> H <sub>5</sub> O <sub>2</sub> <sup>+</sup>		0.28
	83.050	C <sub>5</sub> H <sub>7</sub> O <sup>+</sup>		1.81
	95.050	C <sub>6</sub> H <sub>7</sub> O <sup>+</sup>		0.67
	107.085	C <sub>8</sub> H <sub>11</sub> <sup>+</sup>		0.26
	109.065	C <sub>7</sub> H <sub>9</sub> O <sup>+</sup>		0.36
	109.101	C <sub>8</sub> H <sub>13</sub> <sup>+</sup>		0.43
nopinone	121.102; 139.112	C <sub>9</sub> H <sub>15</sub> O <sup>+</sup>	15 <sup>d</sup> –79 <sup>c</sup>	6.5
	139.137	C <sub>10</sub> H <sub>19</sub> <sup>+</sup>		1.23
	140.114	no match		0.54
m153	153.092	C <sub>9</sub> H <sub>13</sub> O <sub>2</sub> <sup>+</sup>	1.9 <sup>d</sup> –2.8 <sup>a</sup>	0.35
m155	155.105	C <sub>9</sub> H <sub>15</sub> O <sub>2</sub> <sup>+</sup>	0.8 <sup>a</sup> –5.3 <sup>d</sup>	0.51
m185	185.115	C <sub>10</sub> H <sub>17</sub> O <sub>3</sub> <sup>+</sup>	0.1 <sup>a</sup> –0.5 <sup>d</sup>	0.26

## A dynamic plant chamber system with downstream reaction chamber

J. Timkovsky et al.

Title Page

Abstract

Introduction

Conclusions

References

Tables

Figures

◀

▶

◀

▶

Back

Close

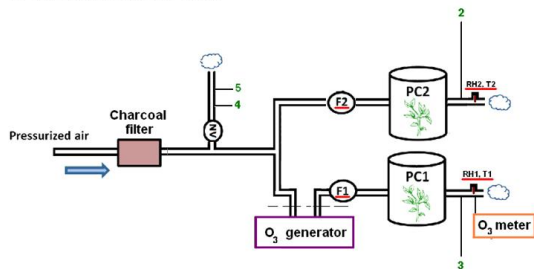
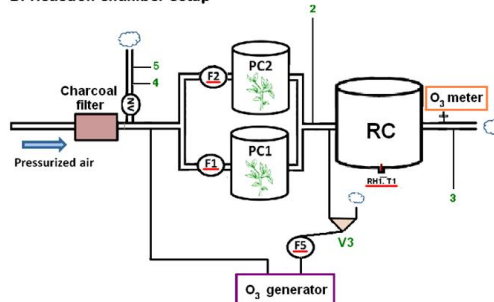
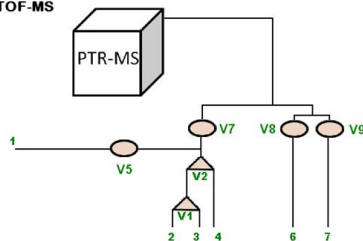
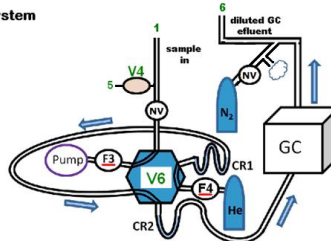
Full Screen / Esc

Printer-friendly Version

Interactive Discussion

**Table 3.** Average night and day emission rates of birch seedlings. Daytime light levels were 130–150  $\mu\text{mol m}^{-2} \text{s}^{-1}$  PAR. Day and night temperatures were  $21.5 \pm 0.2$  and  $20.2 \pm 0.2$  °C, respectively; “–” corresponds to no emission at night.

Compound or $m/z$	Formula $\text{H}^+$	Night emissions, $\text{ng h}^{-1} \text{g}^{-1} \pm \text{SD}$	Day emissions, $\text{ng h}^{-1} \text{g}^{-1} \pm \text{SD}$
41.038	$\text{C}_3\text{H}_5^+$	$15.3 \pm 5.4$	$28.1 \pm 6.7$
43.018	$\text{C}_2\text{H}_3\text{O}^+$	$27.6 \pm 10.4$	$61.0 \pm 15.7$
43.054	$\text{C}_3\text{H}_7^+$	$6.0 \pm 2.6$	$12.5 \pm 2.9$
45.033	$\text{C}_2\text{H}_5\text{O}^+$	$65.9 \pm 28.6$	$150.9 \pm 46.2$
59.049	$\text{C}_3\text{H}_7\text{O}^+$	$91.7 \pm 19.5$	$192.5 \pm 52.6$
61.029	$\text{C}_2\text{H}_5\text{O}_2^+$	$12.2 \pm 11.0$	$23.7 \pm 13.1$
63.044	$\text{C}_2\text{H}_7\text{O}_2^+$	$3.7 \pm 3.3$	$7.3 \pm 3.6$
69.070	$\text{C}_5\text{H}_9^+$	–	$10.7 \pm 5.7$
71.049	$\text{C}_4\text{H}_7\text{O}^+$	$12.3 \pm 5.6$	$39.5 \pm 20.6$
71.085	$\text{C}_5\text{H}_{11}^+$	–	$5.8 \pm 2.3$
85.064	$\text{C}_5\text{H}_9\text{O}^+$	–	$19.4 \pm 8.4$
87.045	$\text{C}_4\text{H}_7\text{O}_2^+$	–	$9.1 \pm 2.8$
87.081	$\text{C}_5\text{H}_{11}\text{O}^+$	–	$8.8 \pm 3.3$
monoterpenes	$\text{C}_{10}\text{H}_{17}^+$	$30.7 \pm 40.4$	$93.9 \pm 72.0$

**A. Dual plant chamber setup****B. Reaction chamber setup****C. PTR-TOF-MS****D. GC-system**

**Fig. 1.** Schematic overview of the setup with two optional chamber configurations (**A** and **B**), PTR-TOF-MS connections (**C**) and GC sampling system (**D**). Port numbers 2, 3 and 4 indicate the sampling positions for the PTR-TOF-MS. The GC samples through port 1 and the GC-effluent is analyzed with the PTR-TOF-MS through port 6. Lab air is analyzed through port 7 and port 5 connects the GC system to purified air for cleaning. The following abbreviations were used: NV – needle valve, PC1, PC2 – plant chambers; RC – reaction chamber, GC – gas chromatograph; V1-V5 and V7-V9 – 2-way (circles) and 3-way (triangles) valves, V6 is a 6-port Valco valve; F1, F2, F3, F4 – flow controllers; RH1, RH2, T1, T2 – temperature and relative humidity sensors; CR1, CR2 – sampling and focusing cryotrap; N<sub>2</sub>, He – nitrogen and helium cylinders; small clouds depict overflow outlets. The parameters which are underlined in red are recorded during measurements.

## A dynamic plant chamber system with downstream reaction chamber

J. Timkovsky et al.

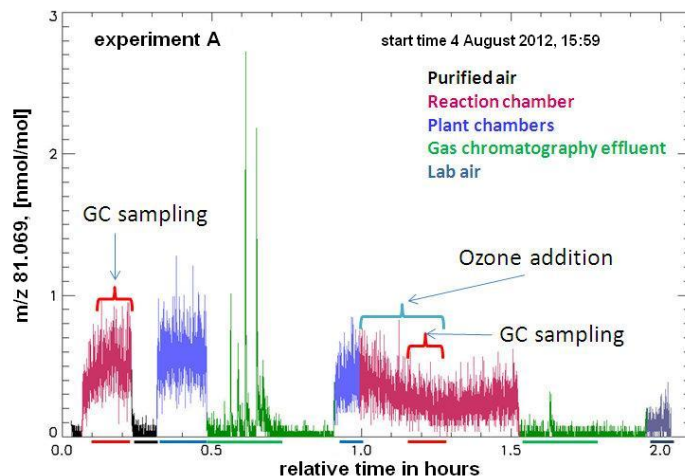


**Fig. 2.** The standard two-hour cycle of measurements. The signal observed at  $m/z$  81.069 is shown as an example, and the color indicates what is measured at a given moment (see legend). The brackets in the plot area indicate GC sampling and ozone addition periods. Colored lines under the x axis depict the averaging/integration period for averaged/integrated data as used in Fig. 3 and 7: last 7 min of first reaction chamber air, last 4 min of purified air, last 9 min of plant chamber air, last 9 min of second plant chamber air, last 7 min of second reaction chamber air (ozone treatment).

[Title Page](#)[Abstract](#)[Introduction](#)[Conclusions](#)[References](#)[Tables](#)[Figures](#)[◀](#)[▶](#)[◀](#)[▶](#)[Back](#)[Close](#)[Full Screen / Esc](#)[Printer-friendly Version](#)[Interactive Discussion](#)

## A dynamic plant chamber system with downstream reaction chamber

J. Timkovsky et al.

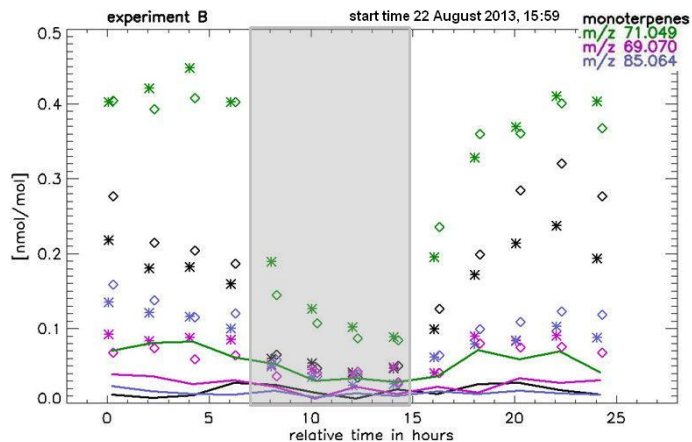


**Fig. 3.** Online measured mixing ratios in the plant chambers (diamonds) and in the reaction chamber without ozone addition (asterisks), experiment B. The respective background levels (purified air) are shown as continuous lines. The shaded area indicates the dark period.

[Title Page](#)[Abstract](#)[Introduction](#)[Conclusions](#)[References](#)[Tables](#)[Figures](#)[◀](#)[▶](#)[◀](#)[▶](#)[Back](#)[Close](#)[Full Screen / Esc](#)[Printer-friendly Version](#)[Interactive Discussion](#)

## A dynamic plant chamber system with downstream reaction chamber

J. Timkovsky et al.

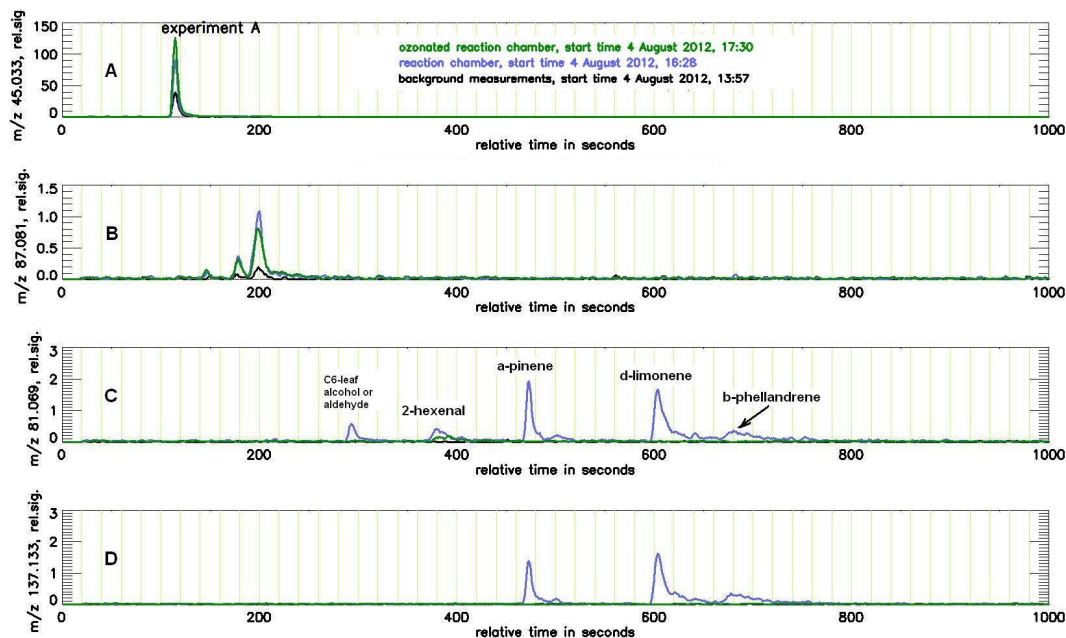


**Fig. 4.** Example gas chromatograms of experiment A. For every profile running mean over 5 points is used. The green line and the blue line correspond to sampling the ozonated and non-ozonated reaction chamber, respectively. The black line is a background chromatogram.  $m/z$  45.033 corresponds to acetaldehyde,  $m/z$  87.081 to methyl butenol (MBO),  $m/z$  81.069 to monoterpenes and additional compounds,  $m/z$  137.133 to monoterpenes only.

Title Page

Abstract

Introduction

Conclusions

References

Tables

Figures

◀

▶

◀

▶

Back

Close

Full Screen / Esc

Printer-friendly Version

Interactive Discussion

## A dynamic plant chamber system with downstream reaction chamber

J. Timkovsky et al.

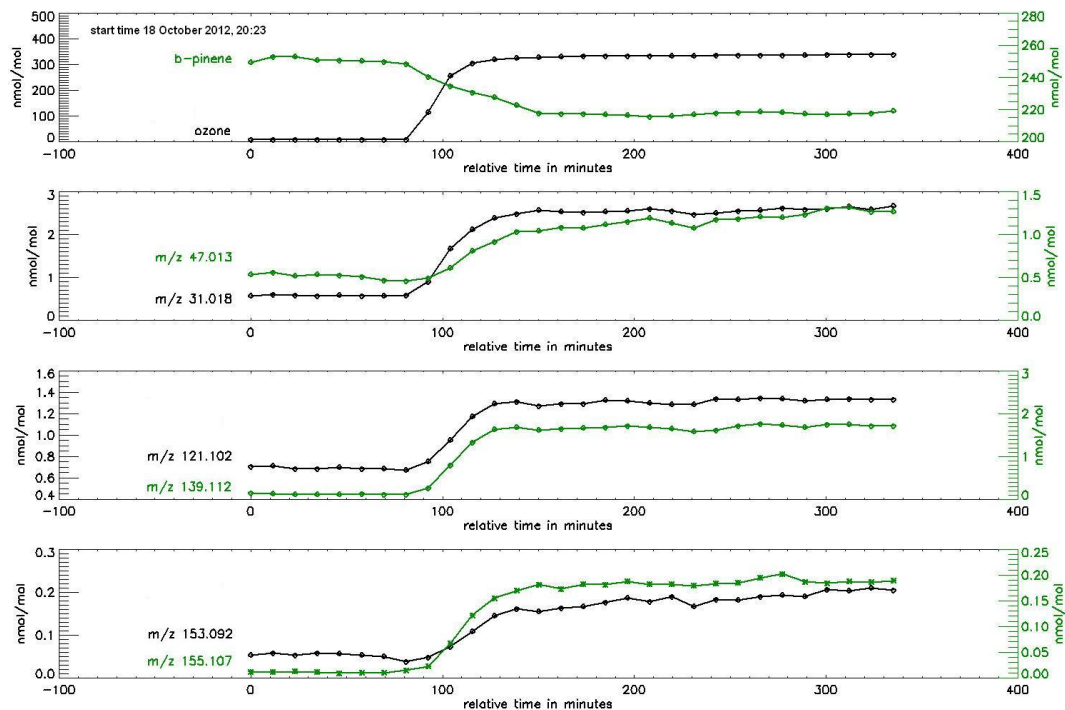


**Fig. 5.** Ozonolysis of  $\beta$ -pinene. The top panel shows the course of ozone and  $\beta$ -pinene (sum of  $m/z$  81.069 and 137.133). The lower panels show oxidation products detected at  $m/z$  31.018 (formaldehyde), 47.013 (formic acid), 121.102 and 139.112 (attributed to nopinone), 153.092 ( $C_9H_{13}O_2^+$ ), and 155.107 ( $C_9H_{15}O_2^+$ ). Ozone was added to the reaction chamber 85 min after the start of the measurements. Presented points are averaged mixing ratios of 11.5 min time periods, which corresponds to the residence time of the air in the reaction chamber.

## A dynamic plant chamber system with downstream reaction chamber

J. Timkovsky et al.

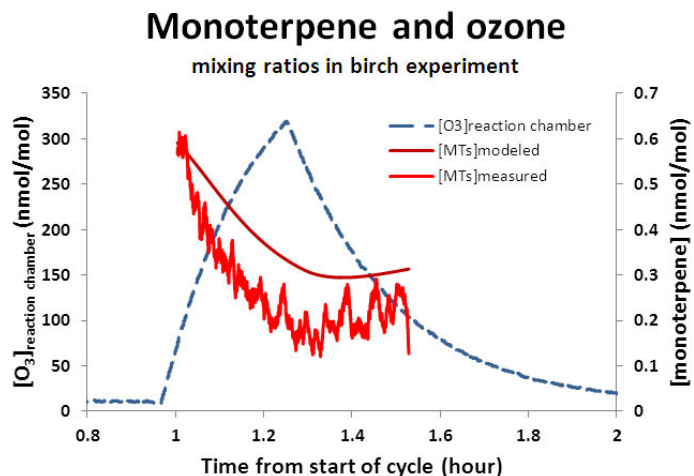


**Fig. 6.** Measured and modeled monoterpene and ozone profiles.  $[O_3]_{\text{reaction chamber}}$  is the ozone mixing ratios in the reaction chamber.  $[MTs]_{\text{measured}}$  corresponds to the monoterpene mixing ratios in the reaction chamber;  $[MTs]_{\text{calculated}}$  corresponds to the monoterpene mixing ratios in the reaction chamber calculated as described in Sect. 3.3. Presented measured monoterpene data are averaged over 2 min.

[Title Page](#)
[Abstract](#)
[Introduction](#)
[Conclusions](#)
[References](#)
[Tables](#)
[Figures](#)
[⏪](#)
[⏩](#)
[◀](#)
[▶](#)
[Back](#)
[Close](#)
[Full Screen / Esc](#)
[Printer-friendly Version](#)
[Interactive Discussion](#)

## A dynamic plant chamber system with downstream reaction chamber

J. Timkovsky et al.

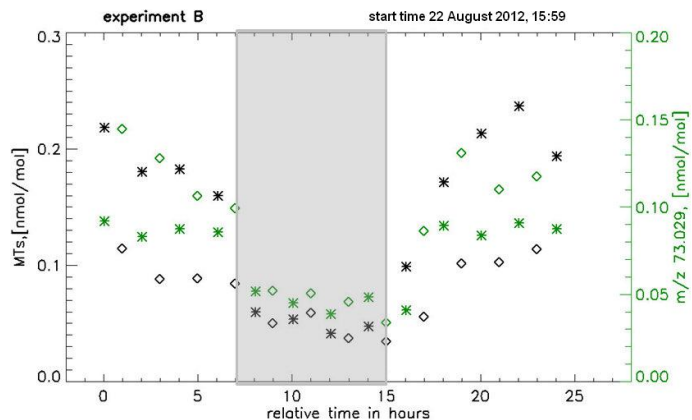


**Fig. 7.** Online measured mixing ratios of monoterpenes (MTs) and  $m/z$  73.029 in the reaction chamber without ozone addition (asterisks) and during/after ozone addition (diamonds), experiment B. The shaded area indicates the dark period.

[Title Page](#)[Abstract](#)[Introduction](#)[Conclusions](#)[References](#)[Tables](#)[Figures](#)[◀](#)[▶](#)[◀](#)[▶](#)[Back](#)[Close](#)[Full Screen / Esc](#)[Printer-friendly Version](#)[Interactive Discussion](#)